

## REVIEWS

### Drug Delivery

E. Guisasola, A. Baeza, L. Asín,  
J. M. de la Fuente,  
M. Vallet-Regí\* ..... 1800007

**Heating at the Nanoscale through  
Drug-Delivery Devices: Fabrication and  
Synergic Effects in Cancer Treatment  
with Nanoparticles**



**Nanoparticles acting as “hot spots”** can achieve both killing of cancer cells and triggering thermoresponsive drug-delivery devices without a global temperature rise. The synthesis, heating mechanisms, and applications are discussed along with the synergic effect of nanoscale hyperthermia and chemotherapy, which can be done with these sorts of devices.

# Heating at the Nanoscale through Drug-Delivery Devices: Fabrication and Synergic Effects in Cancer Treatment with Nanoparticles

Eduardo Guisasola, Alejandro Baeza, Laura Asín, Jesús M. dela Fuente, and María Vallet-Regí\*

Nanocarriers for cancer therapy have been extensively studied, but there is still some research that must be addressed in order to achieve their safe application. In this field, hyperthermia thermal treatments mediated by the use of responsive nanomaterials are not different, and researchers have carried out many attempts to overcome their drawbacks due to the valuable potential of these techniques. Here, an overview is presented of nanodevices based on magnetic- and photoresponsive nanocrystals that respond to magnetic fields and/or near-infrared stimuli for cancer therapies. Special attention is given to the synergic effect that can be achieved with nanoscale heating in combination with chemotherapy through drug-delivery devices to effectively kill cancer cells. In this way, the nanoparticles act as heating sources or “hot spots,” which can trigger cellular responses in the absence of a global temperature rise, making the tumor cells more sensitive to chemotherapeutics. The fabrication of optical and magnetic drug-delivery devices, the heating mechanisms, and their applications in tumor treatment are also summarized.

## 1. Introduction

Hyperthermia thermal treatments have been practiced for their antitumor effect using not very sophisticated but effective technologies, such as saunas and hot water baths.<sup>[1]</sup> The knowledge

that cancer cells are more sensitive to heat than normal ones<sup>[2,3]</sup> and the huge advances in the field of nanotechnology have given researchers new tools to design new, more sophisticated, and more specific heat treatments. Here, we focus on several electromagnetic responsive nanomaterials capable of acting as thermostats, which can induce changes in their environment through heating processes. We will pay special attention to the heat generation and its applications, as well as the biological response to the temperature rise at the nanoscale. Two sorts of nanomaterials that allow these new thermal-treatment approaches are especially attractive, depending on the radiation used to provoke the nanomaterial's response. Answering to the type of radiation used to carry out hyperthermia treatments, the


nanomaterial characteristics required are completely different. The first application is typically called magnetic hyperthermia (MH), which uses alternating magnetic fields (AMFs); which are electromagnetic (EM) waves in the range of the EM spectrum that corresponds to radiofrequency (RF). The second, typically called optical hyperthermia, uses radiation in the part of the EM spectrum that corresponds to the near-infrared (NIR).

The first approaches in hyperthermia treatments in both optical and magnetic stimuli mediated by nanoparticles were focused on the idea of using high doses of nanomaterials to produce enough heat to kill cancer cells by a global temperature increase. Researchers working in this field have to face several drawbacks, as the difficulty of localizing a high concentration of material in the target tissue, inadequate animal models, inaccurate temperature measurement, or limitations of the source conditions that can be used for in vivo experiments make the temperature rise often insufficient.<sup>[4]</sup>

First, it is important to consider that the half-life and tissue penetration of the nanocarrier does not depend on the nanoparticle nature but on the coatings developed to enhance their stability in the physiological environment. Therefore, besides the heating efficiency, the predominant factor in the choice of hyperthermia generation is restricted by the location of the cancer tissue. Both RF and NIR irradiation can be considered useful external and noninvasive stimuli, but the main difference between the two is the tissue penetration. While magnetic fields

Dr. E. Guisasola, Dr. A. Baeza, Prof. M. Vallet-Regí  
Dpto. Química Inorgánica y Bioinorgánica  
Instituto de Investigación Sanitaria Hospital 12 de Octubre  
i+12 Universidad Complutense de Madrid  
Plaza Ramon y Cajal s/n, 28040 Madrid, Spain  
E-mail: vallet@ucm.es

Dr. E. Guisasola, Dr. A. Baeza, Dr. L. Asín, Dr. J. M. de la Fuente,  
Prof. M. Vallet-Regí  
Centro de Investigación Biomédica en Red de Bioingeniería  
Biomateriales y Nanomedicina (CIBER-BBN)  
Av. Monforte de Lemos, 3-5. Pabellón 11. Planta 0, 28029 Madrid, Spain  
Dr. E. Guisasola  
Biomolecular Nanotechnology Group  
CIC BiomaGUNE  
Paseo Miramón 182, 20014 Donostia-San Sebastián Spain  
Dr. L. Asín, Dr. J. M. de la Fuente  
Instituto de Ciencia de Materiales de Aragón  
CSIC-Universidad de Zaragoza  
C/ Pedro Cerbuna 12, 50009 Zaragoza, Spain

 The ORCID identification number(s) for the author(s) of this article can be found under <https://doi.org/10.1002/smt.201800007>.

DOI: 10.1002/smt.201800007

in the RF range can pass through the whole body, near-infrared lasers can only penetrate a few centimeters into the tissues. If the cancer location is deep inside the body, light irradiation must be done during a surgical procedure (e.g., laparoscopy), which makes this method no longer noninvasive. Regarding the heating efficiency, both systems are fully dependent on the nanoparticle nature, size, and chosen technical parameters (laser power and irradiated area for gold nanoparticles (GNPs), and magnetic field frequency and amplitude for magnetic nanoparticles (MNPs)). In this way, the huge range of possibilities that can be afforded prompt one to think that the necessary heating efficiency can be achieved by both systems.

In recent years, new approaches for thermal therapy have been designed and many studies have been carried out, where new heating agents are developed and their efficacy is probed, either alone or in combination with other antitumor treatments such as radiotherapy or chemotherapy, trying to achieve a synergetic effect among them. By using this sublethal or mild hyperthermia, the material amount and experimental parameters are not so aggressive. In this way, the heat generated is not enough to cause a macroscopic temperature increase but a localized heating is achieved, the so-called “hot spots.” Despite the fact that hot spots are not enough to increase the macroscopic temperature, they trigger some cellular responses and sensitize the cells, making them more sensitive to other stimuli, such as drugs. Krawczyk et al. demonstrated that mild hyperthermia leads to a degradation of BRCA2, a protein involved in a DNA repair mechanism known as homologous recombination, which repairs double-strand DNA breaks. Being deficient in this DNA repair mechanism makes cells more sensitive to drugs that provoke DNA damage, which is one of the reasons why heating makes cells more sensitive to many chemotherapeutic agents.<sup>[5]</sup> As will be further described, the biological effects that are studied in both hyperthermia systems are: i) changes in the plasmatic membrane function, ii) activation of thermally sensitive proteins, and iii) the overexpression of some proteins. However, when combining with drug release, a general cytotoxic effect is the most common analyzed parameter.

## 2. Nanomaterials as Thermosteeds

To develop suitable nanocarriers for drug delivery it is necessary to entrap therapeutic molecules in a matrix that also acts as a stabilization moiety in biological fluids, which can be achieved through the functionalization of inorganic nanoparticles. This decoration can be carried out by ligand exchange or encapsulation processes with different moieties, such as polymers, silica, or small molecules. The therapeutic molecules can be retained by electrostatic, hydrophobic, or hydrogen-bond interactions, as well as labile bonds.<sup>[6,7]</sup> The retention time should be long enough to release the drug molecules once the devices are accumulated in the diseased tissue. In general, the thermosteeds act as heating sources, which triggers the drug release through the heat transfer to an external thermoresponsive moiety. This goal can be achieved in different ways, such as breaking thermolabile bonds (between the drug and the thermosteed or degrading the matrix structure), inducing a conformational change in the matrix, or disrupting the matrix structure during the AMF/NIR application.<sup>[8]</sup>



**Alejandro Baeza** received his Ph.D. at Universidad de Alcalá in 2007 developing a novel total synthesis of marine alkaloids. During 2008–2009, he completed a postdoctoral stay in the group of Prof. Ben Feringa (Nobel Prize of Chemistry 2016) at Groningen University (The Netherlands) working in the development of Wacker-type

oxidations. Since 2009, he has been a senior researcher in chemistry in the Pharmaceutical Sciences department at Complutense University in Madrid. His research interests are focused on nanomaterials for antitumoral applications, with special interest in the development of stimuli-responsive nanocarriers and novel targeting moieties able to enhance the selectivity of the nanomedicines against tumoral tissues.



**Jesus M de la Fuente** (Barakaldo-Spain) finished his Ph.D. work in 2003, working on the evaluation of carbohydrate–carbohydrate interactions using gold nanoparticles at the Institute of Chemical Research from CSIC. Once he obtained his Ph.D., he moved to the Centre for Cell Engineering, University of Glasgow (UK) for two years

to develop a research project involving the development of nanoparticles and their biological application. In June 2007, he established the Nanotherapy and Nanodiagnostic Group at the University of Zaragoza. Since 2014, he has been a permanent researcher at the Spanish National Research Council—Aragon Materials Science Institute (Spain).



**María Vallet Regí** is a full professor of inorganic chemistry at Complutense University (Madrid). She is recognized as pioneer in the application of silica mesoporous materials to biomedicine, especially in bone-tissue engineering and controlled drug release.

### 2.1. Magnetic Nanoparticles

The magnetic field required for MH applications is an exceptional stimulus due to its noninvasive character, high penetration in tissues, and magnetic-heating capability. It also can be

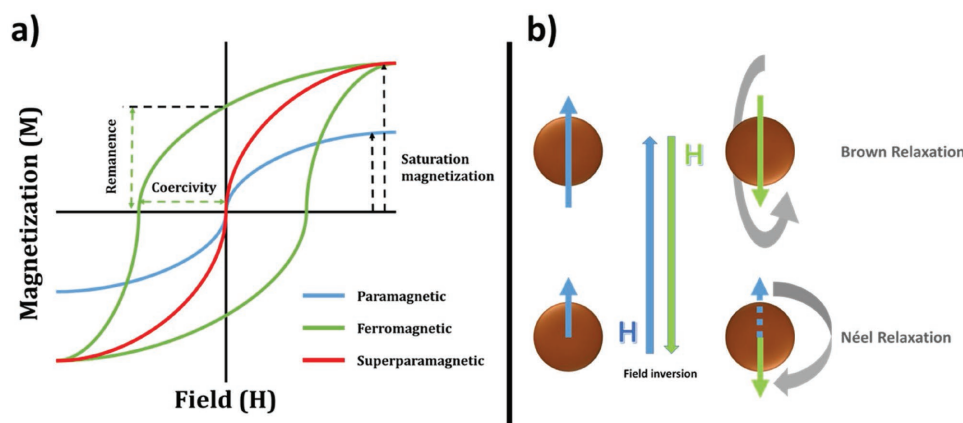


**Figure 1.** a) Magnetization curves obtained using a vibrating sample magnetometer (VSM) for different magnetic materials. b) Magnetic moment change in the relaxation processes of Brown and Néel.

used to enhance the signal intensity in magnetic resonance imaging (MRI), leading to a high degree of soft-tissue contrast, depth of penetration, and spatial resolution.<sup>[9]</sup> The interaction between the magnetic fields and MNPs reveals this to be a powerful tool for biomedical diagnosis and treatment, e.g., in gene transfection or MNP localization.<sup>[10–12]</sup>

The special features of MNPs arise from their structure, size, and composition. These properties lead to different magnetic states. For example, in paramagnetic materials the magnetic moments are randomly aligned, which results in a zero net magnetization. Nevertheless, ferromagnetic bulk materials possess different magnetic domains in which the magnetic moments are uniformly directed. These sorts of materials possess magnetic multidomains in their structures.

In the case of superparamagnetic materials, the size reduction of the nanoparticles forces them to minimize their magnetic energy, adopting a single magnetic domain above a certain temperature called the blocking temperature ( $T_B$ ). The characteristic magnetization curve of superparamagnetic nanoparticles shows a lack of hysteresis with a high saturation magnetization, which ensures a great and rapid response to a magnetic field (Figure 1).

The heating process of these nanoparticles involves the application of an AMF. When MNPs are subjected to a magnetic field, the magnetic moment of each nanoparticle aligns with the field direction. The AMF application implies a rapid field inversion, which forces the superparamagnetic MNPs to change the orientation of their magnetic moment. This fact causes energy losses, mainly by two different relaxation effects, when the nanoparticles relax back to the original magnetic field state. In the presence of an AMF, the magnetic moments rotate, provoking heat dissipation through the Néel relaxation. If the particles are free to rotate, the friction of their surfaces with the surrounding medium also produces a heating effect due to Brownian relaxation.

Several parameters participate in the heating capacity of the MNPs, such as composition, size distribution, nanoparticle coating, and magnetic field amplitude and frequency. The specific absorption rate (SAR) also called the “specific loss power” (SLP) measures the heating efficiency of MNPs under a specific magnetic field frequency ( $f$ ) and dispersant medium

(Equation (1)). It established the rate between the energy absorbed per unit mass of nanoparticles, where  $C$  is the specific heat capacity of the dispersant and  $\Delta T/\Delta t$  is the temperature change of the sample during the AMF application.<sup>[13]</sup> To report the heating efficiency the “intrinsic loss power” is also used because it is nearly independent of the frequency and intensity of the applied AMF<sup>[14]</sup>

$$\text{SAR (or SLP)} = C \cdot (\Delta T/\Delta t) [\text{Wg}^{-1}] = f \times (\text{Hysteresis loop area}) \quad (1)$$

Commonly, the magnetic nanoparticles are composed of metallic elements (Fe, Co, Ni), oxides ( $\text{MgFe}_2\text{O}_4$ ,  $\text{Mn}_3\text{O}_4$ ), alloys ( $\text{CoPt}_3$ , FePt), and even nitrides (FeN). Considerable attention has been paid to iron oxide nanoparticles, especially in ferrite colloids, such as magnetite ( $\text{Fe}_3\text{O}_4$ ) and maghemite ( $\gamma\text{-Fe}_2\text{O}_3$ ), because of their biodegradability and biocompatibility, which make them excellent candidates for medical and pharmaceutical applications.<sup>[15]</sup> Many different methods have been described to synthesize monodisperse and highly stable magnetic nanoparticles. These methods can be classified into three main synthesis pathways: i) physical routes, ii) wet chemistry methods, and iii) microbial synthesis. **The first pathway englobes the physical size reduction to the nanometer scale,** electron-beam lithography, or vapor deposition, between others.<sup>[16,17]</sup> Unluckily, these methods lack control over the average particle size; however, other physical techniques, such as laser ablation, have been found to obtain a good size distribution for MNPs of 20–50 nm using coarse materials.

The wet-chemical preparations are widely used for synthesis of MNPs. The most used methods are: i) chemical coprecipitation of metal ions, ii) thermal decomposition of organometallic compounds, iii) hydrothermal reactions, and iv) microemulsions. These approximations allow highly stable nanoparticles to be obtained with different shapes and a narrow size distribution. Besides, the versatility of these pathways has led to the development of many other techniques, which are greatly described in the recent literature.<sup>[18]</sup>

Interesting advances have also been made in magnetic coatings to develop bimagnetic core-shell structures. The modulation of the core and shell dimensions regulates the interfacial exchange interaction between the two magnetic phases and

allows precise control over the magnetic properties of these core-shell nanoparticles.<sup>[19]</sup> Regarding the microbial synthesis, magnetic nanoparticles are obtained by a biomineralization route carried out by magnetotactic bacteria through a slow crystal growth process. In this way, single-domain or multi-domain nanoparticles between 20–45 nm can be produced in high yields, with reproducibility and good control over the composition and size of the MNPs.<sup>[20]</sup> The synthetic path does not end at this point. In order to use nanoparticles as thermal seeds for drug-delivery platforms, it is necessary to coat these particles with functional entities that provide the devices with stability in a physiological environment.

Superparamagnetic behavior is a requirement of biomedical applications because, in the absence of a magnetic field, they do not retain their magnetization (remanence), by which aggregation after field removal is avoided. Also, the low dipole-dipole interactions help toward the stability of the nanoparticles. This colloidal stability can be improved by functionalization of MNPs with protective agents that take the advantage of electrostatic and steric repulsion to enhance their half-life in different media.<sup>[18]</sup> For biomedical applications, the usual size of superparamagnetic nanoparticles has been ~~stablish~~ approximately between 10 and 50 nm. In this way, many magnetic nanovehicles have been fabricated so far, taking advantage of the covalent and noncovalent relations of the MNPs with the carrier matrices and other functionalities. These coatings can improve several properties, such as the device stabilization, the drug-loading efficiency, the pharmacokinetics, and even confer on-demand release characteristics.

One of the most used carrier moieties is polymer coatings. The versatility of polymer formulations has allowed different hybrid drug-delivery devices to be built through different approaches. For example, the direct grafting of polymer chains to the surface of an MNP permits the design of a polymer moiety prior to the attachment or the growing step,<sup>[21]</sup> while the formation of magnetic micelles with amphiphilic polymers by encapsulation of MNPs represents a less complex synthetic procedure.<sup>[22]</sup> Tuning the hydrophilic/hydrophobic interactions between polymer chains, the formation of magnetic polymerosomes is also possible.<sup>[23]</sup> In this case, the MNPs can be carried in the hydrophobic crust or in the hydrophilic core, depending on the nature of the nanoparticle coating. Moreover, some of these examples are capable of retaining chemotherapeutic agents with different hydrophilic/hydrophobic natures either by noncovalent interactions or labile bond formation, achieving different drug-delivery kinetics.<sup>[8,24]</sup>

Similar supramolecular interactions have been also used to fabricate magnetic nanocarriers, forming a lipid bilayer that entraps the MNPs inside, called magnetoliposomes.<sup>[25]</sup> In fact, the widely known commercial formulation Doxil utilizes this technique of organization for the delivery of doxorubicin.

Important developments have also been achieved with inorganic porous materials. The most significant can be those made with mesoporous silica nanoparticles (MSNs).<sup>[26]</sup> The porous structure, together with its easy surface functionalization process, lead to several magnetic sensitive drug-delivery nanocarriers by their cleavable bonds, thermoresponsive polymer coatings, or the disruption of supramolecular interactions.<sup>[27–33]</sup> This kind of device has been also used to confirm the hot-spot

effect, pointed out recently by several research groups.<sup>[34–36]</sup> Dong and co-workers used rare-earth nanocrystals as nanothermometers to measure the temperature at the nanoscale inside MSNs, together with iron oxide nanoparticles.<sup>[37]</sup> The heat generation produced by AMF application, induced a rise in the fluorescence signal of the nanothermometer, which was measured and related accurately to the temperature inside (and outside) the nanodevice. The same year, Guisasaola et al. demonstrated that these nanocarriers are capable of releasing their cargo without increasing the global temperature under AMF application.<sup>[38]</sup> In this case the MNPs were encapsulated inside MSNs and a thermoresponsive polymer coating was employed to retain the cargo. The AMF application was carried out in isothermal conditions at 37 °C with a water recirculating system in the sample holder, mimicking physiological conditions. The accelerated release of the cargo was achieved only when the AMF was applied, showing that the heat produced by the MNPs was capable of overcoming the heat dissipation and triggering the cargo release by thermoresponsive polymer activation.

## 2.2. Gold Nanoparticles

The use of GNPs as thermal seeds in photothermal therapy has been widely studied in the past years due to the excellent optical properties of these systems, such as high absorption and scattering in the EM spectrum region, which comprises the visible (390–650 nm) to NIR region (650–1350 nm).<sup>[39]</sup> GNPs present surface plasmon resonance (SPR) when they are exposed to a light source with a specific wavelength, which is dependent on the size and shape of the particle. SPR appears as a consequence of the interaction that light presents with free electrons in the plasmon band located on the metal surface. This interaction induces a polarization in the electronic density, which oscillates accordingly with the wavelength of the incident light (**Figure 2a**).<sup>[40]</sup> These excited electrons lose the gained energy by electron-electron scattering followed by heat transfer to the surroundings by phonon-phonon interactions.<sup>[41]</sup> When the particle is symmetric on all axes, as is the case for spherical ones, only one SPR adsorption band appears, at around 520 nm, whereas in the case of gold nanorods (GNRs), a second SPR band is presented due to the existence of two oscillation modes along each axis of the particle (longitudinal and transversal).<sup>[42]</sup> The location of this second band is always placed at a higher frequency, and it is strongly dependent on the particle aspect ratio (length to width) relation. Thus, the location and intensity of this second band can be tuned by the variation of the particle aspect ratio. Gold nanorods with aspect ratio higher than 2 present a strong SPR band in the NIR region (**Figure 2b**).

Light in the visible region is rapidly adsorbed by living tissues, especially caused by the presence of hemoglobin, which presents an intense adsorption band in this region. On the contrary, when the light wavelength corresponds to the NIR region, it can penetrate into the tissues, reaching zones up to 10 cm deep due to the high transparency of the components of the tissues to this radiation. The capacity of these GNRs to convert NIR into heat has been widely studied and can even be monitored by spectroscopic methods such as time-resolved IR spectroscopy.<sup>[43]</sup>



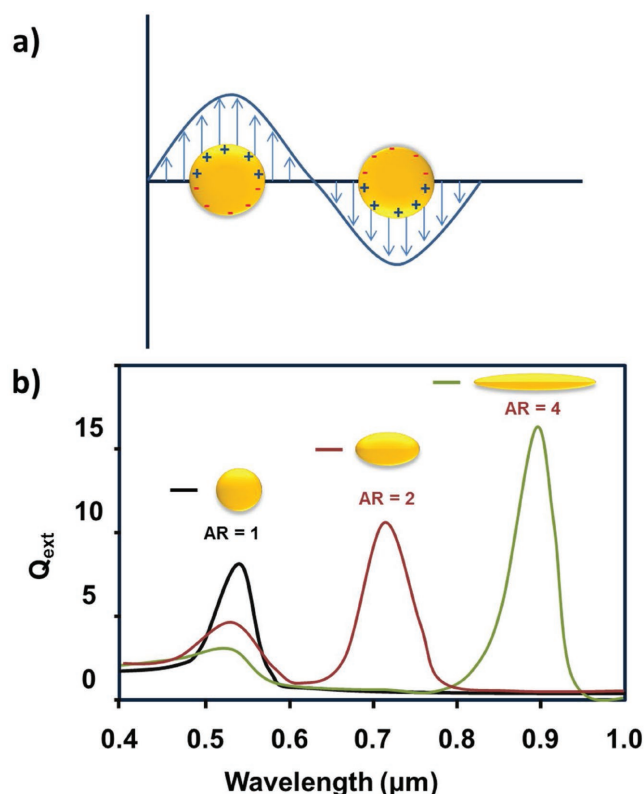


**Figure 2.** a) Interaction of electrons on the particle surface with light. b) SPR bands of gold nanoparticles depending of their shape.

The synthesis of GNRs and the important parameters that control their aspect ratio have been widely studied elsewhere.<sup>[39]</sup> These GNRs can be produced with a precise shape control by several methods, such as photochemical<sup>[44]</sup> and electrochemical synthesis,<sup>[45]</sup> being one of the most employed procedures, the seed-mediated approach.<sup>[46]</sup> This last method is based on the chemical reduction of gold salts to obtain gold seeds with a diameter around 3–4 nm. These seeds are then added to a solution containing a weak reductor, more gold salts, and a surfactant as a stabilizer and structure-directing agent, usually cetyltrimethylammonium bromide (CTAB). Thus, GNRs are formed by anisotropic growth on the gold seeds. This method provides GNRs with relatively high colloidal stability in aqueous solution thanks to the formation of a CTAB coating positively charged on the rod surface. The biological application of these rods requires the removal of this CTAB coating due to the high toxicity of this compound in the micromolar range. CTAB has been replaced by different small molecules, such as phosphatidylcholine<sup>[47]</sup> and polymers such as polyelectrolyte-based coatings<sup>[48]</sup> or poly(ethylene glycol) (PEG) chains. The nanoparticle surface decoration with this last polymer (PEG) has received huge attention because nanoparticles coated with PEG are less prone to be captured by the cells of mononuclear phagocyte system and, therefore, their circulation time into the bloodstream is significantly higher than that of naked ones. The PEG layer forms a hydrophilic barrier by which the adhesion of opsonins is avoided; these are proteins with the function of labeling foreign bodies for allowing the macrophages to capture and destruct them. Niidome et al. have functionalized

GNRs with PEG<sub>5000</sub>-SH using the great affinity of thiols for the gold surface.<sup>[49]</sup> The resulting GNR-PEG showed very low cytotoxicity, even at high concentrations up to  $0.5 \times 10^{-3}$  M and prolonged circulation time within the bloodstream. El-Sayed et al. demonstrated the antitumoral capacity of GNR-PEG using an in vivo squamous cell carcinoma mice model.<sup>[50]</sup> The administration of these particles, followed by NIR irradiation in the tumoral zone, induced 57% of tumoral resorption if the particles were directly injected in the tumoral lesion and 25% of resorption in the case of intravenous injection. Other polymeric-based coatings have also been employed. As an example, Fucoidan is a natural polymer obtained from marine brown algae, which, besides demonstrating excellent biocompatibility, biodegradability and low cost, presents antibacterial, antitumoral, and antiviral activity. This highly negatively charged polymer binds to the GNR surface by electrostatic interactions with the CTAB placed on the surface, considerably reducing the GNR cytotoxicity. Low-molecular-weight glycans have been anchored on GNRs, being capable of providing high colloidal stability and also the capacity to recognize tumoral cells, because these moieties are able to selectively bind to certain membrane receptors overexpressed by tumoral cells.<sup>[51]</sup> The external surface of the rods can be electrostatically functionalized with specific antibodies, such as Anti-EGFR, in order to localize, in a selective manner, the GNR into the tumoral cells.<sup>[52]</sup> Other macromolecules that have been used as targeting moieties are aptamers. Aptamers are DNA or RNA single or double strands that adopt a characteristic tridimensional structure, which allows binding to specific tumoral cell membrane receptors. Cheng et al. employed GNRs decorated with KW16-13 aptamer for the selective destruction of MCF10CA1h human breast ductal carcinoma cells.<sup>[53]</sup> The heat produced by the exposition of the cells with internalized GNR to NIR can damage the macromolecular cell machinery causing the destruction of the cell, especially those cells which produce low amount of the proteins responsible for the defense against temperature increases such as heat shock proteins (HSP70 or BAG3, among others).<sup>[54]</sup> The external surface of GNRs has been decorated with a positively charged poly(diallyldimethylammonium chloride), which retains a specific RNA capable of silencing the expression of BAG3.<sup>[55]</sup> The combined effect of heat induction and gene silencing significantly enhances the cellular damage after NIR irradiation. Chen et al. have studied the use of polyethylene imine (PEI) for coating the GNR surface, in order to transport oligonucleotide sequences, and reported that PEI with a molecular weight of 11.8 kDa is the best system for clinical applications, because it presents a nice balance between transfection efficacy and low toxicity.<sup>[56]</sup> Oncolytic viruses, which are pathogens that mainly attack tumoral cells, have been administered in combination with GNRs because it has been demonstrated that the temperature increase generated by GNRs under NIR irradiation enhances the cellular virus uptake and its expression within the target cell.<sup>[57]</sup> Guerrero-Martínez et al. reported the use of GNRs functionalized with PEG in their sides for providing colloidal stability to the system and ( $\pm$ )- $\alpha$ -lipoic acid at the tips of the nanorods.<sup>[58]</sup> When the GNRs were engulfed by the tumoral cells, the mild acidic conditions presented in the late endosomes/lysosomes (pH = 5) induced the protonation of the lipoic acid causing a tip-to-tip aggregation of the

GNRs. The formation of these oligomers caused a change in the GNR aspect: ratio which allowed the temperature to be increased using NIR lasers with lower power than in the case of single nanorods (down to  $0.21 \text{ W cm}^{-2}$ ). This value is maintained below the maximum permissible exposure threshold of skin, which corresponds to  $0.4 \text{ W cm}^{-2}$ , being suitable for clinical applications. Plasmonic properties can be easily tuned using more gold nanosystems with exotic shapes, such as gold nanodendrites, which have proved that the capacity to destroy tumoral cells can be improved by modification of the degree of branching, being optimal in the case of low branching.<sup>[59]</sup>

When a nanoparticle is injected into the bloodstream, it is immediately coated with different blood proteins, forming the so-called protein corona. This corona can compromise the selectivity of the nanodevices because it hides the targeting moieties. However, the formation of this corona can also be employed as a targeting moiety or as drug transporter itself. Kah et al. described the use of GNRs coated with a protein corona of human serum in which a photosensitizer (Chlorin e6) was loaded.<sup>[60]</sup> The excitation at 665 nm generated fivefold-times-higher reactive oxidant species compared with free sensitizer, resulting in practically complete tumoral cell destruction at low dosages in the nanomolar range.

Despite this section being focused on optical hyperthermia through NIR irradiation of gold nanocrystals, other important materials are used in photothermal therapies. A wide variety of nanomaterials also demonstrates excellent photothermal effects by NIR application, such as carbon quantum dots, graphene, and even polymers.<sup>[61–63]</sup>

### 3. Hot-Spot Effect—From a Biological Point of View

#### 3.1. Magnetic Hyperthermia

In the bibliography, we can find that an appreciable part of biological effects observed in MNP-loaded cells exposed to AMF are described at the membrane level. Some of the studies use cells that express thermosensitive proteins, and the effect of the released heat is studied by analyzing the function of the protein involved. Some examples of this idea are given by Huang et al., who made in vitro and in vivo studies with a nanomaterial consisting of manganese ferrite NPs functionalized with streptavidine molecules. The cells they worked with (HEK 293) were genetically modified to express a transmembrane protein modified with biotin, which results in the MNPs being located at the plasmatic membrane. Three different fluorophores were used to detect the temperature changes at different locations: in the surrounding of the MNPs, inside the cells, and in the solution. By measuring the fluorescence intensity as a molecular-scale temperature probe, they demonstrated that when MNPs were bounded to the plasmatic membrane and cells were submitted to an AMF, the generated heat was limited to the vicinity of the MNPs. After 15 s, **the heat was limited to the plasma membrane remaining unmodified the intracellular temperature.** The cell line also expressed a thermosensitive protein (TRPV1) and they also demonstrated that these hot spots were able to remotely activate TRPV1, enhancing the amount of intracellular

$\text{Ca}^{2+}$ . They performed some in vivo studies with *Caenorhabditis elegans* worms showing the remote triggering of a behavioral response. More specifically, the worms change their locomotion when they suffer from heat, and they demonstrated that MNP-loaded worms showed this alteration when exposed to an AMF.<sup>[64]</sup> Stanley et al. engineered cells to express a thermally sensitive modified ion channel (TRPV1) and a  $\text{Ca}^{2+}$ -dependent insulin construct. Cells were targeted with MNPs coated with a specific antibody (anti-TRPV1). By submitting them to AMF, membrane hot spots lead the cells to gate  $\text{Ca}^{2+}$ , which produces an increase in insulin production, **leading to a decrease in sugar blood concentration** during in vivo conditions.<sup>[65]</sup>

Other studies have demonstrated that cells treated with MH suffer from toxicity even when the released heat is not enough to increase the macroscopic temperature.<sup>[66,67]</sup> Trying to better understand the cellular effects that take place in MH and to be able to distinguish between macroscopic heating and localized heating, some methods have been developed. Moros et al. analyzed the expression of heat shock proteins (HSP70) through in vitro **an** in vivo experiments, and they observed that even **the** macroscopic temperature did not change during the MH treatment, the protein HSP70 was overexpressed, and the levels achieved in both systems were comparable to the levels obtained when external heating experiments were carried out at a temperature of  $12^\circ\text{C}$  higher than the basal conditions.<sup>[68]</sup> Furthermore, Mukherjee et al. used a temperature-dependent construct as a reporter for comparing macroscopic hyperthermia and nanoparticle-mediated hyperthermia. The construct consisted of a heat shock element promoter that controlled the expression of luciferase enzyme. The results showed that cellular stress was observed at mild hyperthermia conditions when no cell death was observed, both in macroscopic heating and nanoscale heating with MNPs. Interestingly, cellular stress was also observed in MH experiments when cells with NPs but without the reporter system were in contact with cells with the reporter system but without NPs, revealing a bystander effect.<sup>[69]</sup> Calatayud et al. also showed that when cells without MNPs and without AMF exposure were in contact with MH treated cells, there existed a bystander effect that affected the cell viability of the former ones.<sup>[70]</sup> Recently, Stocke et al. compared heat effects and structural changes in 3D micrometastatic tumor analogs when they were incubated with high ( $1 \text{ mg mL}^{-1}$ ) and low ( $0.1 \text{ mg mL}^{-1}$ ) doses of MNPs. They reported that cells incubated with a low dose of MNPs and exposed to AMF showed a high cytoplasmatic vacuolization and precipitation of extracellular debris indicating autophagy process. On the other hand, cells incubated with the high dose of MNPs and exposed to AMF presented higher accumulation of MNPs and higher cell-death rates but not cytoplasmatic vacuolization. Interestingly, they also showed a higher intracellular accumulation of MNPs in cells exposed to AMF compared to the unexposed ones.<sup>[71]</sup> With all these results, we can conclude that by exposing cells loaded with MNPs to AMF, it is possible to obtain hot spots that heat only the vicinity of the MNPs and dissipate very fast, not observing an elevation of the macroscopic temperature. As the experimental parameters are so different between groups, different biological effects have been observed, from expression of proteins to cell death. It seems clear that there are still many studies that need to be done in order to deeply evaluate the



effects of MNPs in mild or sublethal hyperthermia conditions. Standardization of experimental methodology would be of interest, as it will allow a better comparison of results between different groups.

### 3.2. Optical Hyperthermia

Other types of experiments are focused on the strategy of generating heat with light in order to control some cellular functions. For this purpose, NPs with the capability of absorbing energy from light should be used, as has been discussed above. The NPs mostly used for this purpose in biological studies are gold NPs, but there are others like graphene NPs that have been also studied. Many studies have been made to elucidate the effect that a dramatic increase of the temperature, very typically observed with gold NPs, has at the plasmatic membrane level. In this line of research, Li et al., trying to understand the photothermally enhanced gold NPs' intracellular delivery, reported that when exposing a single gold NP in the vicinity of the plasmatic membrane to a laser beam, a rapid temperature increase and the formation of nanobubbles were observed, resulting in the formation of a transient hole where the NPs enter into the cell.<sup>[72]</sup> The same effect of nanobubble formation is observed when gold NPs are clustered in cells and exposed to a laser beam. Taking advantage of this phenomenon, Lukianova-Hleb et al. used gold NPs to mechanically inject extracellular cDNA plasmid to enhance the effectiveness of the gene therapy process in vitro.<sup>[73]</sup> Another effect observed at the cellular membrane level is the change in the electrical resistance and in the current flow. Urban et al. demonstrated that the local heating produced by gold NPs in contact with a cell membrane was enough to vary the amount of current passing through the bilayer membrane, varying its permeability.<sup>[74]</sup> In addition, Carvalho-de-Souza et al. demonstrated that neurons could be stimulated in the presence of gold NPs when subjected to a laser pulse, resulting in the production of an action potential. When NPs were functionalized with some ligand molecules, they could be used to repetitive stimulations resisting convective washouts.<sup>[75]</sup> Carrying on with the effect that gold nanomaterials could have in contact with cells, Nakatsuji et al. demonstrated that gold nanorods could photothermally induce  $\text{Ca}^{2+}$  influx solely by TRPV1 activation, and not by membrane damage, depending on the functionalization of the nanorods.<sup>[76]</sup> Recently, Marino et al. showed how they can remotely activate striated muscle cells by inducing myotube contraction with gold nanoshells when they are internalized by cells and exposed to a near-infrared laser. They also demonstrated that several modulating related genes are overexpressed.<sup>[77]</sup>

In conclusion, there is evidence that several effects, at the membrane level, can be triggered by the high temperatures reached by gold NPs when exposed to laser pulses, such as changes in their electrical properties like the alteration of membrane capacitance, changes in their permeability resulting in the formation of transient membrane holes, and, when cells have been previously genetically modified and express any thermosensitive protein, changes in ions flux can be also observed.

## 4. Joining Together Hot Spots and Drug Release: Synergistic Effects from a Biological Point of View

As has been previously mentioned, there are some approaches that combine the effect caused by the heat generated by any of the hyperthermia treatments and the effect triggered by other drugs, such as chemotherapeutic agents, as can be seen in Figure 3. When talking about hyperthermia and drug release, MH may be the one that takes the best advantage of the synergistic effect because, usually, the heat released by magnetic particles when submitted to an AMF is not enough to provoke a macroscopic temperature increase to kill cancer cells for in vivo conditions. For this reason, new approaches combining MH with drug release have been developed in order to achieve a high cytotoxic effect. On the other hand, despite optical hyperthermia being able to release a higher amount of heat, some approaches, in combination with drug release, have been carried out in order to develop a synergistic effect, increasing the potency of the thermal killing effect and decreasing the systemic toxicity of some chemotherapeutic agents. To achieve a selective drug release in combination of the hyperthermia approach, the use of thermosensitive polymers is of a great importance. The idea of using this kind of polymers is to take advantage of the heat released by nanomaterials when exposed to suitable radiation to make the drug-release system very specific and externally controlled.

### 4.1. Magnetic Hyperthermia and Drug-Release Applications

Different combinations of MNPs and chemotherapeutic agents have been described in the literature; some recent examples are mentioned here and the analyzed biological effects are revised. Recently, Zhang et al., proposed the use of a nanomaterial

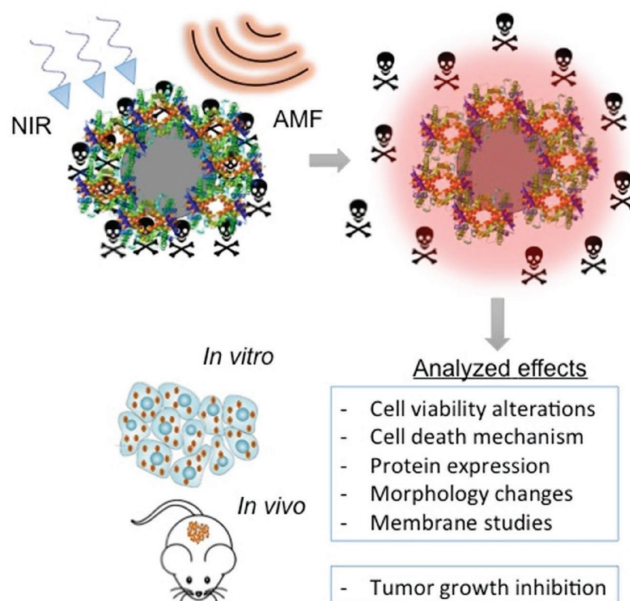


**Figure 3.** Scheme representing the general idea of the combination of hyperthermia treatment and drug release. The most studied effects both for in vitro and in vivo experiments are listed.



consisting of poly(organophosphazene)-based hydrogels charged with iron-oxide-based MNPs and tumor-necrosis-factor-related apoptosis-inducing ligand (TRAIL) to achieve a high antitumor activity by MH treatments. The heat released by MH treatment increases the temperature of the hydrogel above 43 °C, provoking the dissolution of the hydrogel, and subsequently TRAIL molecules are released. In vitro experiments were carried out by exposing different group of cells to two cycles of MH heating up to 43 °C. The results showed that cell viability only decreased in cells that contained the nanomaterial loaded with TRAIL. Apoptotic cell death and overexpression of caspase 3 were detected. In vivo results showed a high antitumor effect in a group of mice containing the material with TRAIL after two MH cycles, in comparison with the control groups. Thus, despite a considerable macroscopic heating existing, the authors used the term “mild hyperthermia” because cells without the drug were not affected by the treatment.<sup>[78]</sup>

Another study that uses TRAIL molecules as antitumoral agent was carried out by Yin et al., who used Zn-doped magnetite nanoparticles to form complexes between these MNPs and a heat-inducible plasmid construct that codifies for the TRAIL ligand. With these complexes, they achieved both delivery by magnetofection and activation of the expression of TRAIL in mesenchymal cells by mild MH. In vitro studies have reported that TRAIL is expressed and released to the medium by mesenchymal transfected cells. A supernatant of these cells was able to decrease the cell viability of ovarian cancer cells. In addition, in vivo results have shown that mesenchymal cells activated by mild MH **have already the capability to home tumors.**<sup>[79]</sup>

The combination of hybrid nanogels containing MNPs and a drug like curcumin was studied by Cazares et al. These nanogels consisted of a polymer matrix (based on oligo(ethylene glycol) methyl ether methacrylate, **OEGMA**), which has a conformational transition at 47 °C and entraps both MNPs and curcumin molecules. In vitro studies demonstrated that PC3 cells were able to internalize these gels and 2 h after the exposition to an AMF, the cell viability of the group of cells with the gel-DOX was lower than of all the control groups, due to the enhanced intracellular DOX release. It is noteworthy that the macroscopic temperature did not increase during the MH treatment.<sup>[80]</sup>

Seidel et al. studied the antitumoral efficacy of nanomaterials consisting of iron-oxide-based MNPs covered with a silica layer and functionalized with a thermolabile linker modified with an antitumor toxin (derived from ansamitocin). In vitro studies showed that cell proliferation was decreased when MNP-loaded cells were subjected to an AMF. In vivo experiments reflected that, despite the fact that tumor temperatures increased up to 43 °C, the treatment efficiency in the group of mice with the nanomaterial and the drug was enough to provoke the inhibition of tumor growth in comparison with the control groups. Anatomopatologic studies revealed that tumor cells expressed Ki67, a typical marker for cell proliferation, and terminal deoxynucleotidyl transferase dUTP nick end labeling (TUNEL) staining revealed an increase in apoptosis.<sup>[81]</sup>

## 4.2. Optical Hyperthermia and Drug-Release Applications

Some examples of studies of the synergistic effect of optical hyperthermia and drug release as an antitumor treatment are

discussed in this section. You et al. showed that gold nanospheres loaded with doxorubicin were accumulated in the tumor area in a higher dose than free doxorubicin when injected intravenously in mice. They explained this effect by the enhanced permeability and retention effect of tumors. They also showed a higher antitumor effect when irradiating the tumor with an NIR laser compared to free doxorubicin, nanomaterial without laser exposure, and liposomal doxorubicin.<sup>[82]</sup> Another study with the same chemotherapeutic agent was carried out by Zhang et al. They performed in vivo experiments and demonstrated that doxorubicin-loaded graphene oxide, when injected intravenously and submitted to an NIR laser had a synergistic antitumoral effect compared to free doxorubicin and graphene oxide without drug but exposed to an NIR laser.<sup>[83]</sup> Zhang et al. developed a nanomaterial that consisted of a thermosensitive gel loaded with both GNRs and paclitaxel. The heat produced by the GNRs when applying an NIR laser provoked both cellular thermal ablation and the release of the drug to enhance the antitumoral effect of the combined treatment, observing a synergistic effect when compared to single treatments, as observed in the previous studies. By an infrared camera, they showed how the temperature in the spot where the laser was placed increased up to 69 °C, whereas it decreased sharply to the non-irradiated region.<sup>[84]</sup> Lu et al. studied the synergistic effect of nanoplateforms based on periodic mesoporous organosilica and CuS particles and doxorubicin. They also observed that internalization of the materials was enhanced by photothermal treatment, in accordance with previous authors who claimed that the membrane suffers changes in its viscosity and permeability due to thermal treatment. In vivo studies at mild hyperthermia conditions, 41–42 °C, revealed a synergistic effect of thermal treatment and doxorubicin release in tumor growth when compared to single treatments.<sup>[85]</sup> There are also some studies comparing different heat-treatment mechanisms, such as Yuan et al., who compared the cell viability at the same thermal dose when heating with a water bath and when heating using heat-inductive materials in nanocomposites. Their results revealed that the cell viability decrease achieved by the photothermal treatment was higher than the effect observed in cells heated using a water bath. These effects were observed at mild hyperthermia conditions in heat-resistant cells such as MCF7.<sup>[86]</sup>

In addition, there are some studies that present nanomaterials in combination with both magnetic nanoparticles and particles for optical hyperthermia, such as that of Wang et al., which have recently proposed the use of nanomaterials based on magnetite-based MNPs, carbon dots, silica, and paclitaxel. MNPs were used as magnetic resonance contrast agents and carbon dots as heating agents in optical hyperthermia using NIR radiation. The heat released triggered paclitaxel release and in vivo experiments showed that combined treatment, chemotherapy and thermal therapy, resulted in a higher tumor-growth decrease compared to single treatments. They attributed this effect to the increase of drug release, cell permeability and enhanced drug internalization under NIR radiation.<sup>[87]</sup> Another example of nanomaterials in this research line is that proposed by Ma et al., consisting of nanoellipsoids with a magnetite core and a silica-based shell, where GNRs are attached and doxorubicin is loaded. As in the previous study, the MNPs served as contrast agents for MRI, and the GNRs were the heating agents

in optical hyperthermia. In vivo results showed an enhanced antitumor efficiency when using this material, compared with the use of drug or thermal treatment alone.<sup>[88]</sup>

In conclusion, it can be said that the most studied biological effects to evaluate the efficacy of these types of MH treatments are cell viability (by many different cytotoxic tests) during in vitro experiments and tumor growth inhibition during in vivo experiments. However, in some of them, a more detailed studied about the death mechanism can be seen, as shown in Figure 3.

## 5. Bonus Track: Co-Working between Photo- and Magnetic Heating: Magneto-Plasmonic Nanohybrids for Hyperthermia

The two modalities described here can effectively be merged in a single device: both MH and photothermal heating. Magnetic-plasmonic combination has been recently pioneered by Espinosa and co-workers through maghemite multicore-shaped nanoparticles with gold shells around the magnetic core.<sup>[89]</sup> This device was coated with poly(vinylpyrrolidone) since the synthesis steps and its biocompatibility and tumor cell capture were definitely tested in vivo. The results showed a high efficiency in MH and tunable plasmonic properties in the NIR region of the gold shell in a mouse animal model. Then, the multimodal device achieves a rapid temperature rise of the tumor tissue to 48 °C with a ten times lower dose than classical MH treatment. It is also remarkable that the gold shell on the multicore superparamagnetic iron oxide nanoparticles (SPIONs) can prevent the fast intracellular degradation of the iron oxide nanocrystals, which allows efficient heat delivery.<sup>[90]</sup>

Besides the use of gold (plasmonic) and iron oxide (magnetic) nanocrystals is the understandable path for the development of such thermo-therapy, many different materials have been used to combine both therapies. A variety of devices comprising magnetic nanoparticles capped with photoresponsive polymers to more complex magnetic mesoporous silica nanoparticles capped with graphene quantum dots have been recently described. Thus, this approximation has proved its potential by combining MH, photothermal therapy (PTT), chemotherapy, and even imaging in vitro and in vivo, which makes them excellent candidates for multimodal treatment of cancer.<sup>[91–94]</sup>

## 6. Conclusion

In recent years, a great number of different nanodevices that are able to generate localized hyperthermia and controlled drug release under the application of external stimuli have been developed for antitumoral therapy. These smart nanosystems provide a significant efficacy improvement over conventional therapy, as has been widely described here. The core of these nanodevices (mainly inorganic) interacts with the applied external stimuli, either light radiation or magnetic fields, generating a heat shock that fires ingenious triggering mechanisms of temperature-responsive coatings, allowing drug release. More research is needed to improve the efficacy of these nanodevices regarding achieving a more sensitive response under the application of low-intensity stimuli compatible with their

clinical application. Playing with different geometries and sizes of the sensitive cores, developing novel metallic alloys or nanocrystals with stronger heat production, or designing smarter temperature-responsive coatings, among others, could be ways to reach the final clinical target.

Concerning in vitro studies, some biological effects have been described as consequence of a localized and moderate heat treatment, as has been reviewed here. These effects go from the changes observed at the plasmatic membrane level, passing through the expression of heat shock proteins to the different mechanisms of cell death. Other types of effects using more sophisticated and genetically modified cells have been described, supporting localized heating application. In vivo studies have shown and demonstrated the synergistic effect between heat and drug therapy, and the parameter analyses in these kinds of experiments are, in general, the inhibition of the tumor growth or the prolongation of survival rate. Thus, better knowledge is needed to understand the dynamics of the cell response to heating at the nanoscale and the synergic effect with chemotherapeutic agents. The lack of consensus regarding the experimental parameters of the stimuli exposition and the rest of the methodology makes it difficult to compare results between different groups. It is also of great importance to study in detail the accumulation in the tumor area and the final fate of these nanosystems after different administration routes and their biological effects within living hosts at long times, especially in the case of nonbiodegradable materials such as gold or certain metallic alloys. There is plenty of room to improve the performance and biocompatibility of these nanomaterials, which will provide, with no doubt, important tools in the fight against this terrible disease.

## Acknowledgements

This work was supported by the European Research Council (Advanced Grant VERDI; ERC-2015-AdG Proposal No. 694160, and Proof of Concept HOTFLOW; ERC-2016-POC Proposal No. 754609), the project MAT2015-64831-R, the project SAF2014-54763-C2-2-R, Fondo Social de la DGA (grupos DGA). L.A. acknowledges the Juan de la Cierva Program for her postdoctoral position.

## Conflict of Interest

The authors declare no conflict of interest.

## Keywords

drug delivery, hot spots, magnetic hyperthermia, near-infrared hyperthermia, stimuli-responsive materials

Received: January 11, 2018

Revised: February 26, 2018

Published online:

[1] E. S. Glazer, S. A. Curley, *Surg. Oncol. Clin. North Am.* **2011**, *20*, 229.

[2] B. Woodhall, K. L. Pickrell, G. N. G. M. S. Mahaley, H. T. Dukes, *Ann. Surg.* **1960**, *151*, 750.

- [3] G. M. Hahn, **1974**, 3117.
- [4] A. Jordan, R. Scholz, P. Wust, H. Föhling, R. Felix, *J. Magn. Magn. Mater.* **1999**, 201, 413.
- [5] P. M. Krawczyk, B. Eppink, J. Essers, J. Stap, H. Rodermond, H. Odijk, *Proc. Natl. Acad. Sci. USA* **2011**, 108, 9851.
- [6] M. Vallet-Regí, F. Balas, D. Arcos, *Angew. Chem., Int. Ed.* **2007**, 46, 7548.
- [7] M. W. Tibbitt, J. E. Dahlman, R. Langer, *J. Am. Chem. Soc.* **2016**, 138, 704.
- [8] K. Ulbrich, K. Holá, V. Šubr, A. Bakandritsos, J. Tuček, R. Zbořil, *Chem. Rev.* **2016**, 116, 5338.
- [9] M. A. Busquets, J. Estelrich, M. J. Sánchez-Martín, *Int. J. Nanomed.* **2015**, 10, 1727.
- [10] S. Carregal-Romero, E. Caballero-Díaz, L. Beqa, A. M. Abdelmonem, M. Ochs, D. Hühn, B. S. Suau, M. Valcarcel, W. J. Parak, *Annu. Rev. Anal. Chem.* **2013**, 6, 53.
- [11] N. Sun, Z. Liu, W. Huang, A. Tian, S. Hu, *Crit. Rev. Oncol. Hematol.* **2014**, 89, 352.
- [12] A. Singh, S. K. Sahoo, *Drug Discovery Today* **2014**, 19, 474.
- [13] A. Kolhatkar, A. Jamison, D. Litvinov, R. Willson, T. Lee, *Int. J. Mol. Sci.* **2013**, 14, 15977.
- [14] R. R. Wildeboer, P. Southern, Q. A. Pankhurst, *J. Phys. D: Appl. Phys.* **2014**, 47, 495003.
- [15] M. Arruebo, R. Fernández-Pacheco, M. R. Ibarra, J. Santamaría, *Nano Today* **2007**, 2, 22.
- [16] R. Arbain, M. Othman, S. Palaniandy, *Miner. Eng.* **2011**, 24, 1.
- [17] J. G. King, W. Williams, C. D. W. Wilkinson, S. McVitie, J. N. Chapman, *Geophys. Res. Lett.* **1996**, 23, 2847.
- [18] L. H. Reddy, J. L. Arias, J. Nicolas, P. Couvreur, *Chem. Rev.* **2012**, 112, 5818.
- [19] M. Hammad, V. Nica, R. Hempelmann, *IEEE Trans. Magn.* **2017**, 53, 1.
- [20] J. Baumgartner, L. Bertinetti, M. Widdrat, A. M. Hirt, D. Faivre, *PLoS One* **2013**, 8, 1.
- [21] M. Pernia Leal, A. Torti, A. Riedinger, R. La Fleur, D. Petti, R. Cingolani, R. Bertacco, T. Pellegrino, *ACS Nano* **2012**, 6, 121116140336006.
- [22] J.-H. Fang, Y.-H. Lai, T.-L. Chiu, Y.-Y. Chen, S.-H. Hu, S.-Y. Chen, *Adv. Healthcare Mater.* **2014**, 3, 1250.
- [23] S.-H. Hu, B.-J. Liao, C.-S. Chiang, P.-J. Chen, I.-W. Chen, S.-Y. Chen, *Adv. Mater.* **2012**, 24, 3627.
- [24] S. H. Hu, S. Y. Chen, X. Gao, *ACS Nano* **2012**, 6, 2558.
- [25] R. Di Corato, G. Béalle, J. Kolosnjaj-Tabi, A. Espinosa, O. Clément, A. K. A. Silva, C. Ménager, C. Wilhelm, *ACS Nano* **2015**, 9, 2904.
- [26] E. Aznar, M. Oroval, L. Pascual, J. R. Murguía, R. Martínez-Máñez, F. Sancenón, *Chem. Rev.* **2016**, 116, 561.
- [27] A. Baeza, E. Guisasola, E. Ruiz-Hernández, M. Vallet-Regí, *Chem. Mater.* **2012**, 24, 517.
- [28] P. Saint-Cricq, S. Deshayes, J. I. Zink, A. M. Kasko, *Nanoscale* **2015**, 7, 13168.
- [29] J. Liu, C. Detrembleur, M.-C. De Pauw-Gillet, S. Mornet, L. Vander Elst, S. Laurent, C. Jérôme, E. Duguet, *J. Mater. Chem. B* **2014**, 2, 59.
- [30] Y. Zhu, C. Tao, *RSC Adv.* **2015**, 5, 22365.
- [31] C. Tao, Y. Zhu, *Dalton Trans.* **2014**, 43, 15482.
- [32] Y. Xu, Y. Zhu, S. Kaskel, *RSC Adv.* **2015**, 5, 99875.
- [33] X. Yu, Y. Zhu, *Sci. Technol. Adv. Mater.* **2016**, 17, 229.
- [34] A. Riedinger, P. Guardia, A. Curcio, M. A. García, R. Cingolani, L. Manna, T. Pellegrino, *Nano Lett.* **2013**, 13, 2399.
- [35] J. T. Dias, M. Moros, P. Del Pino, S. Rivera, V. Grazú, J. M. de la Fuente, *Angew. Chem., Int. Ed. Engl.* **2013**, 52, 11526.
- [36] L. Polo-Corrales, C. Rinaldi, *J. Appl. Phys.* **2012**, 111, 2010.
- [37] J. Dong, J. I. Zink, *ACS Nano* **2014**, 8, 5199.
- [38] E. Guisasola, A. Baeza, M. Talelli, D. Arcos, M. Moros, J. M. De La Fuente, M. Vallet-Regí, *Langmuir* **2015**, 31, 12777.
- [39] J. Pérez-Juste, I. Pastoriza-Santos, L. M. Liz-Marzán, P. Mulvaney, J. Perez-Fuste, I. Pastoriza-Santos, L. Liz-Marzan, P. Mulvaney, *Coord. Chem. Rev.* **2005**, 249, 1870.
- [40] S. Eustis, M. A. El-Sayed, *Chem. Soc. Rev.* **2006**, 35, 209.
- [41] J. Li, J. Liu, C. Chen, *ACS Nano* **2017**, 11, 2403.
- [42] W. Il Choi, A. Sahu, Y. H. Kim, G. Tae, *Ann. Biomed. Eng.* **2012**, 40, 534.
- [43] S. C. Nguyen, Q. Zhang, K. Manthiram, X. Ye, J. P. Lomont, C. B. Harris, H. Weller, A. P. Alivisatos, *ACS Nano* **2016**, 10, 2144.
- [44] F. Kim, J. H. Song, P. Yang, *J. Am. Chem. Soc.* **2002**, 124, 14316.
- [45] Yu, S.-S. Chang, C.-L. Lee, C. R. C. Wang, *J. Phys. Chem. B* **1997**, 101, 6661.
- [46] A. Gole, C. J. Murphy, *Chem. Mater.* **2004**, 16, 3633.
- [47] H. Takahashi, Y. Niidome, T. Niidome, K. Kaneko, H. Kawasaki, S. Yamada, *Langmuir* **2006**, 22, 2.
- [48] T. S. Hauck, A. A. Ghazani, W. C. W. Chan, *Small* **2008**, 4, 153.
- [49] T. Niidome, M. Yamagata, Y. Okamoto, Y. Akiyama, H. Takahashi, T. Kawano, Y. Katayama, Y. Niidome, *J. Controlled Release* **2006**, 114, 343.
- [50] E. B. Dickerson, E. C. Dreaden, X. Huang, I. H. El-Sayed, H. Chu, S. Pushpanketh, J. F. McDonald, M. A. El-Sayed, *Cancer Lett.* **2008**, 269, 57.
- [51] I. García, A. Sánchez-Iglesias, M. Henriksen-Lacey, M. Grzelczak, S. Penadés, L. M. Liz-Marzán, *J. Am. Chem. Soc.* **2015**, 137, 3686.
- [52] P. Manivasagan, S. Bharathiraja, M. Santha Moorthy, Y.-O. Oh, K. Song, H. Seo, J. Oh, *ACS Appl. Mater. Interfaces* **2017**, 9, 14633.
- [53] R. Chandrasekaran, A. S. W. Lee, L. W. Yap, D. A. Jans, K. M. Wagstaff, W. Cheng, *Nanoscale* **2016**, 8, 187.
- [54] M. R. K. Ali, H. R. Ali, C. R. Rankin, M. A. El-Sayed, *Biomaterials* **2016**, 102, 1.
- [55] B.-K. Wang, X.-F. Yu, J.-H. Wang, Z.-B. Li, P.-H. Li, H. Wang, L. Song, P. K. Chu, C. Li, *Biomaterials* **2016**, 78, 27.
- [56] J. Chen, H. Liang, L. Lin, Z. Guo, P. Sun, M. Chen, H. Tian, M. Deng, X. Chen, *ACS Appl. Mater. Interfaces* **2016**, 8, 31558.
- [57] B. K. Jung, Y. K. Lee, J. Hong, H. Ghandehari, C. O. Yun, *ACS Nano* **2016**, 10, 10533.
- [58] R. Ahijado-Guzmán, G. González-Rubio, J. G. Izquierdo, L. Bañares, I. López-Montero, A. Calzado-Martín, M. Calleja, G. Tardajos, A. Guerrero-Martínez, *ACS Omega* **2016**, 1, 388.
- [59] P. Qiu, M. Yang, X. Qu, Y. Huai, Y. Zhu, C. Mao, *Biomaterials* **2016**, 104, 138.
- [60] E. L. L. Yeo, J. U.-J. Cheah, D. J. H. Neo, W. I. Goh, P. Kanchanawong, K. C. Soo, P. S. P. Thong, J. C. Y. Kah, *J. Mater. Chem. B* **2017**, 5, 254.
- [61] Z. Tian, X. Yao, K. Ma, X. Niu, J. Grothe, Q. Xu, L. Liu, S. Kaskel, Y. Zhu, *ACS Omega* **2017**, 2, 1249.
- [62] H. Yamane, K. Tanaka, Y. Chujo, *Polym. J.* **2018**, 50, 271.
- [63] Q. Zhang, Z. Wu, N. Li, Y. Pu, B. Wang, T. Zhang, J. Tao, *Mater. Sci. Eng., C* **2017**, 77, 1363.
- [64] H. Huang, S. Delikanli, H. Zeng, D. M. Ferkey, A. Pralle, *Nat. Nanotechnol.* **2010**, 5, 602.
- [65] S. A. Stanley, J. E. Gagner, S. Damanpour, M. Yoshida, J. S. Dordick, J. M. Friedman, *Science* **2013**, 336, 604.
- [66] M. Creixell, A. C. Bohórquez, M. Torres-Lugo, C. Rinaldi, *ACS Nano* **2011**, 5, 7124.
- [67] L. Asín, G. F. Goya, A. Tres, M. R. Ibarra, *Cell Death Dis.* **2013**, 4, e596.
- [68] M. Moros, A. Ambrosone, G. Stepien, F. Fabozzi, V. Marchesano, A. Castaldi, A. Tino, J. M. de la Fuente, C. Tortiglione, *Nanomedicine* **2015**, 10, 2167.
- [69] A. Mukherjee, M. Castaneres, M. Hedayati, M. Wabler, P. Kulkarni, R. Rodriguez, R. H. Getzenberg, L. Theodore, *Nanomedicine* **2015**, 9, 2729.
- [70] M. R. Calatayud, M. P. Asin, L. Tres, A. Goya, G. F. Ibarra, *Curr. Nanosci.* **2016**, 12, 372.
- [71] N. A. Stocke, P. Sethi, A. Jyoti, R. Chan, S. M. Arnold, J. Z. Hilt, M. Upreti, *Biomaterials* **2017**, 120, 115.
- [72] M. Li, T. Lohmuller, J. Feldmann, *Nano Lett.* **2015**, 15, 770.

- [73] E. Y. Lukianova-hleb, A. P. Samaniego, J. Wen, L. S. Metelitsa, C. Chang, D. O. Lapotko, *J. Controlled Release* **2011**, 152, 286.
- [74] P. Urban, S. R. Kirchner, C. Mühlbauer, T. Lohmüller, J. Feldmann, *Sci. Rep.* **2016**, 6, 22686.
- [75] J. L. Carvalho-de-Souza, J. S. Treger, B. Dang, S. B. H. Kent, D. R. Pepperberg, F. Bezanilla, *Neuron* **2015**, 86, 207.
- [76] H. Nakatsuji, T. Numata, N. Morone, S. Kaneko, Y. Mori, H. Imahori, T. Murakami, *Angew. Chem., Int. Ed.* **2015**, 8501, 11725.
- [77] A. Marino, S. Arai, Y. Hou, A. Degl, V. Cappello, B. Mazzolai, Y. Chang, V. Mattoli, M. Suzuki, G. Ciofani, *ACS Nano* **2017**, 11, 2494.
- [78] Z. Zhang, S. Song, *Biomaterials* **2017**, 132, 16.
- [79] P. T. Yin, S. Shah, N. J. Pasquale, O. B. Garbuzenko, K. Lee, N. Brunswick, *Biomaterials* **2017**, 81, 46.
- [80] E. Cazares-Cortes, A. Espinosa, J. M. Guigner, A. Michel, N. Griffete, C. Wilhelm, C. Ménager, *ACS Appl. Mater. Interfaces* **2017**, 9, 25775.
- [81] K. Seidel, A. Balakrishnan, C. Alexiou, C. Janko, R. M. Komoll, L. L. Wang, A. Kirschning, M. Ott, *Chem. – Eur. J.* **2017**, 23, 12326.
- [82] J. You, R. Zhang, G. Zhang, M. Zhong, Y. Liu, C. S. Van Pelt, D. Liang, W. Wei, A. K. Sood, C. Li, *J. Controlled Release* **2012**, 158, 319.
- [83] W. Zhang, Z. Guo, D. Huang, Z. Liu, X. Guo, H. Zhong, *Biomaterials* **2011**, 32, 8555.
- [84] N. Zhang, X. Xu, X. Zhang, D. Qu, L. Xue, R. Mo, C. Zhang, *Int. J. Pharm.* **2016**, 497, 210.
- [85] N. Lu, P. Huang, W. Fan, Z. Wang, Y. Liu, S. Wang, G. Zhang, J. Hu, W. Liu, G. Niu, R. D. Leapman, G. Lu, X. Chen, *Biomaterials* **2017**, 126, 39.
- [86] J. Yuan, J. Liu, Q. Song, D. Wang, W. Xie, H. Yan, J. Zhou, Y. Wei, X. Sun, L. Zhao, *ACS Appl. Mater. Interfaces* **2016**, 8, 24445.
- [87] H. Wang, K. Wang, B. Tian, R. Revia, Q. Mu, M. Jeon, F.-C. Chang, M. Zhang, *Small* **2016**, 12, 6388.
- [88] M. Ma, H. Chen, Y. Chen, X. Wang, F. Chen, X. Cui, J. Shi, *Biomaterials* **2012**, 33, 989.
- [89] A. Espinosa, M. Bugnet, G. Radtke, S. Neveu, G. A. Botton, C. Wilhelm, A. Abou-Hassan, *Nanoscale* **2015**, 7, 18872.
- [90] F. Mazuel, A. Espinosa, G. Radtke, M. Bugnet, S. Neveu, Y. Lalatonne, G. A. Botton, A. Abou-Hassan, C. Wilhelm, *Adv. Funct. Mater.* **2017**, 27, 1605997.
- [91] H. Yan, W. Shang, X. Sun, L. Zhao, J. Wang, Z. Xiong, J. Yuan, R. Zhang, Q. Huang, K. Wang, B. Li, J. Tian, F. Kang, S.-S. Feng, *Adv. Funct. Mater.* **2018**, 28, 1705710.
- [92] X. Yao, X. Niu, K. Ma, P. Huang, J. Grothe, S. Kaskel, Y. Zhu, *Small* **2017**, 13, 1602225.
- [93] C. Wang, H. Xu, C. Liang, Y. Liu, Z. Li, G. Yang, Y. Li, Z. Liu, F. Nano, *ACS Nano* **2013**, 1, 1.
- [94] C. Li, T. Chen, I. Ocsoy, G. Zhu, E. Yasun, M. You, C. Wu, J. Zheng, E. Song, C. Z. Huang, W. Tan, *Adv. Funct. Mater.* **2014**, 24, 1772.